3D enamel thickness in Neandertal and modern human permanent canines

Laura Buti, Adeline Le Cabec, Daniele Panetta, Maria Tripodi, Piero A Salvadori, Jean-Jacques Hublin, Robin N.M. Feeney, Stefano Benazzi

Journal of Human Evolution 113 (2017) 162–172

Contents lists available at ScienceDirect

Journal of Human Evolution

journal homepage: www.elsevier.com/locate/jhevol

3D enamel thickness in Neandertal and modern human permanent canines

Laura Buti [a, *, 1], Adeline Le Cabec [b, c, 1], Daniele Panetta [e], Maria Tripodi [e], Piero A. Salvadori [e], Jean-Jacques Hublin [b], Robin N.M. Feeney [d], Stefano Benazzi [a, b]

[a] Department of Cultural Heritage, University of Bologna, V. Ariani, 1, 48121 Ravenna, Italy
[b] Department of Human Evolution, Max Planck Institute for Evolutionary Anthropology, Deutscher Platz 6, 04103 Leipzig, Germany
[c] ESRF – The European Synchrotron, 71, Avenue des Martyrs, CS 40220, F-38043 Grenoble Cédex 9, France
[d] UCD School of Medicine, Health Science Centre, University College Dublin, Belfield, Dublin 4, Ireland
[e] Institute of Clinical Physiology – CNR, Via Moruzzi, 1, 56127 Pisa, Italy

ARTICLE INFO

Article history:
Received 31 October 2016
Accepted 3 August 2017

Keywords:
Dental tissue proportions
Micro-CT
3D dental morphology
Average enamel thickness
Relative enamel thickness
Enamel 3D distribution

ABSTRACT

Enamel thickness figures prominently in studies of human evolution, particularly for taxonomy, phylogeny, and paleodietary reconstruction. Attention has focused on molar teeth, through the use of advanced imaging technologies and novel protocols. Despite the important results achieved thus far, further work is needed to investigate all tooth classes. We apply a recent approach developed for anterior teeth to investigate the 3D enamel thickness of Neandertal and modern human (MH) canines.

In terms of crown size, the values obtained for both upper and lower unworn/slightly worn canines are significantly greater in Neandertals than in Upper Paleolithic and recent MH.

The 3D relative enamel thickness (RET) is significantly lower in Neandertals than in MH. Moreover, differences in 3D RET values between the two groups appear to decrease in worn canines beginning from wear stage 3, suggesting that both the pattern and the stage of wear may have important effects on the 3D RET value. Nevertheless, the 3D average enamel thickness (AET) does not differ between the two groups. In both groups, 3D AET and 3D RET indices are greater in upper canines than in lower canines, and overall the enamel is thicker on the occlusal half of the labial aspect of the crown, particularly in MH. By contrast, the few early modern humans investigated show the highest volumes of enamel while for all other components of 3D enamel, thickness this group holds an intermediate position between Neandertals and recent MH.

Overall, our study supports the general findings that Neandertals have relatively thinner enamel than MH (as also observed in molars), indicating that unworn/slightly worn canines can be successfully used to discriminate between the two groups. Further studies, however, are needed to understand whether these differences are functionally related or are the result of pleiotropic or genetic drift effects.

1. Introduction

Enamel thickness is considered a useful dental trait to serve as a proxy for reconstructing life history, diet, taxonomy and behavior of extant and extinct hominoid species (Molnar and Gantt, 1977; Martin, 1983, 1985; Schwartz, 2000a; Martin et al., 2003; Kono, 2004; Grine et al., 2005; Smith et al., 2005, 2008; Olejniczak et al., 2007), particularly within the genus *Homo* (Bayle and Dean, 2011; Smith et al., 2012; Le Luyer et al., 2014). Following early contributions based on the physical sectioning of the tooth (Martin, 1985; Smith et al., 2005, 2006), recent developments entail 2D and mainly 3D digital methods (Olejniczak and Grine, 2006; Olejniczak et al., 2008a,b), which: 1) provide accurate and more objective quantification of enamel thickness, 2) prevent the physical damage of the tooth inherent in physical sectioning and 3) represent a reliable procedure for the inclusion of worn teeth in the analysis, ultimately increasing the sample size of fossil groups.

* Corresponding author.
E-mail addresses: xlaura.buti@gmail.com (L. Buti), adeline_lecabec@mpg.eva.de (A. Le Cabec), daniele.panetta@ifc.cnr.it (D. Panetta), maria.t@email.it (M. Tripodi), piero.salvadori@ifc.cnr.it (P.A. Salvadori), hublin@eva.mpg.de (J.-J. Hublin), robin.feeney@ucd.ie (R.N.M. Feeney), stefano.benazzi@unibo.it (S. Benazzi).
[1] These authors contributed equally to this work.

http://dx.doi.org/10.1016/j.jhevol.2017.08.009

Most studies investigating enamel thickness have focused on molars (Grine, 2002, 2005; Kono et al., 2002; Grine et al., 2005; Kono and Suwa, 2008; Olejniczak et al., 2008c; Skinner et al., 2015). Molars have been widely investigated due to their potential relationship with body size (Martin, 1985), importance in mastication (Molnar and Gantt, 1977; Schwartz, 2000b; Martin et al., 2003; Grine et al., 2005) and the taxonomic information they convey (Bailey, 2002). Furthermore, their morphology allows for the simple application of digital methods (Olejniczak et al., 2008a; Benazzi et al., 2014a; Fornai et al., 2014). Studies of enamel thickness in both deciduous and permanent molars have highlighted significant differences between Neandertals and modern humans (Macchiarelli et al., 2006) and the effectiveness of this parameter to discriminate between the two groups (Olejniczak et al., 2008a). Conversely, little attention has been given to the anterior dentition in these respects, even though front teeth are well preserved in the fossil record, and are sometimes the only tooth class represented in fossil assemblages (e.g., Benazzi et al., 2014b, 2015a; Peretto et al., 2015).

Neandertal anterior teeth have been studied to investigate wear patterns, development and dental loading (Clement et al., 2012), and the canines in particular have been found to be informative relating to their root size and shape (Le Cabec et al., 2012, 2013). Correspondingly, other features, such as enamel thickness distribution, could improve our knowledge of the variation between Neandertal and other human taxa.

The few extensive studies available thus far on enamel thickness variation in canine teeth involve 2D analysis based on physical sections (Schwartz and Dean, 2005; Saunders et al., 2007; Smith et al., 2008) or virtual sections of the 3D rendered models (Feeney et al., 2010; Smith et al., 2012). However, because the 2D enamel thickness is a proxy for the full distribution of the enamel on the crown (i.e., due to the loss of one dimension in 2D; Olejniczak et al., 2008c; Benazzi et al., 2014a), the quantification of 3D enamel thickness is preferred. Few studies, however, have focused on 3D enamel thickness in the anterior teeth, such as for the permanent dentition of the Neandertals from the Sima de las Palomas del Cabezo Gordo (Bayle et al., 2017), for the deciduous teeth of the Neandertal juvenile Spy VI (Crevecoeur et al., 2010) and the modern human child from Abrigo do Lagar Velho (Bayle et al., 2010).

The present study aims to investigate 3D enamel thickness in a sample of Neandertal and modern human upper and lower permanent canines, ranging from unworn to variously worn. Specifically, we sought to: 1) test whether the 3D enamel thickness of canine teeth can discriminate between Neandertals and modern humans and 2) provide new information about enamel thickness distribution in Neandertal and modern human canines.

2. Materials and methods

2.1. Samples

Our total sample comprises 121 permanent upper ($n = 52$) and lower ($n = 69$) canines from Late Pleistocene to extant individuals. The wear stage of the sample was scored following Smith (1984; see Table 1) and ranges from 1 to 2 (unworn-slightly worn), 3 (dentine line of distinct thickness), 4 (moderate dentine exposure no longer resembling a line) and 5 (large dentine area exposed with a complete enamel rim).

The fossil sample consists of Neandertals (NEA = 35) and early modern humans (EMH = 13). The modern human sample consists of Upper Paleolithic and Epi-Paleolithic modern humans (UPMH = 13) and recent modern humans (RMH = 58). The comparative sample of RMH includes teeth derived from clinical extractions, anatomical collections (University of Leipzig Anatomical Collection) and two Italian medieval necropolises from Mantova (Valdaro and Casalmoro). Due to the relatively small UPMH sample size and the lack of significant differences between UPMH and RMH at wear stages 1–2 (see Results), UPMH results are combined with the RMH sample for statistical analysis (hereafter called MH for "modern humans").

Additionally, we have included in our analysis Tabun C2 (Quam and Smith, 1998), the taxonomic attribution of this specimen to Neandertal or early modern human is contentious, and a Combe-Capelle Mesolithic modern human (Hauser, 1924; Hoffmann et al., 2011) to test their enamel thickness components.

Both the fossil material and the RMH comparative sample were selected based on the state of preservation of the crown, including a well preserved cervical line. Specimens presenting pathological conditions, irregular wear facets (e.g., owing to severe malocclusion in the clinical sample), and severe damage in the areas of interest were excluded from the analysis.

2.2. Micro-CT image acquisition and 3D model generation

The majority of the sample was scanned using conventional micro-CT systems at the Max Planck Institute for Evolutionary Anthropology in Leipzig, Germany (a BIR ARCTIS 225/300 industrial micro-CT scanner and a Skyscan 1172 micro-CT scanner) with an isotropic voxel size ranging from 13.7 to 31.67 μm. Details on the scanning parameters are further described in Le Cabec et al. (2013). Synchrotron micro-CT data for the La Quina H18 upper canine (voxel size: 31.12 μm) were obtained from the ESRF (European Synchrotron Radiation Facility, Grenoble, France) paleontological microtomographic database (http://paleo.esrf.eu/picture.php?/378/category/1509, Smith et al., 2010). Data for Equus Cave 9 (EQ 9; Grine and Klein, 1985) were acquired at the ESRF on the ID19 beamline (voxel size: 30.12 μm). The RMH sample from Italy was scanned at the Institute of Clinical Physiology - CNR in Pisa using Xalt, an in-house designed micro-CT scanner, using the following scan parameters: 50 kVp, a 2 mm-thick Al filter, 720 projections over 360°, 0.8 mAs/projection (see further technical details in Panetta et al., 2012). Volumetric data for this latter sample were reconstructed using Feldkamp-type cone-beam filtered back-projection (FBP; Feldkamp et al., 1984) with cubic voxel size of 18.4 μm.

The reconstructed micro-CT images were processed using a semiautomatic threshold-based approach in Avizo 7 (Visualization Sciences Group Inc.) and Seg3D (v2.1.4; http://www.sci.utah.edu/cibc-software/seg3d.html). The segmented enamel cap and virtually filled dentine were converted to meshes using the Windged-Edge Mesh tool of the MeVisLab software (http://www.mevislab.de).

The 3D digital models of the canines were imported in Rapidform XOR2 (INUS Technology, Seoul, Korea; now Geomagic design X: http://www.geomagic.com/it/) for cleaning processes (e.g., removal of triangles not connected to the surface or those that projected beyond the outer surface of the mesh) and correction of defects (e.g., filling of small holes) to create fully closed surfaces necessary for further 3D digital analysis. Following procedures described in Benazzi et al. (2014a), a spline curve was digitized at the cervical line to isolate the coronal dentine, which was then closed by interpolating the curve with a smooth surface (Fig. 1).

2.3. Measuring enamel thickness in 3D

For all teeth, the following variables were quantified following Olejniczak et al. (2008c): volume of the enamel cap ($V_{Enam,}$ in mm^3), volume of the coronal dentine including the coronal pulp ($V_{Dent,}$ in mm^3) and the surface area of the enamel–dentine

Table 1
Permanent lower and upper canines of fossil and extant hominins used in the investigation of 3D enamel thickness.

Taxon	Lower canines						Upper canines					
	Specimen	Side	Wear[a]	Site	Country	Source micro-CT	Specimen	Side	Wear[a]	Site	Country	Source micro-CT
NEA	KRP 51	L	1	Krapina	Croatia	MPI	KRP D102	L	1	Krapina	Croatia	MPI
	KRP 52	R	1	Krapina	Croatia	MPI	KRP D103	L	1	Krapina	Croatia	MPI
	KRP D75	L	1	Krapina	Croatia	MPI	KRP D191	L	1	Krapina	Croatia	MPI
	KRP D120	L	1	Krapina	Croatia	MPI	La Quina H18	L	1	La Quina	France	ESRF
	KRP D121	L	1	Krapina	Croatia	MPI	Scla-4A 16	R	1	Scladina Cave	Belgium	MPI
	Vindija 11-39	R	1	Vindija Cave	Croatia	MPI	KRP D141	R	2	Krapina	Croatia	MPI
	Scla-4A 12[b]	L	1	Scladina Cave	Belgium	MPI	KRP D144	L	3	Krapina	Croatia	MPI
	BD 1	L	2	Abri Bourgeois-Delaunay	France	MPI	KRP D76	R	3	Krapina	Croatia	MPI
	Combe-Grenal I	R	2	Combe-Grenal	France	MPI	KRP D36	R	3	Krapina	Croatia	MPI
	KRP D119	L	2	Krapina	Croatia	MPI	KRP D37	L	3	Krapina	Croatia	MPI
	Le Moustier 1	R	2	Le Moustier	France	MPI	KRP 49	L	3	Krapina	Croatia	MPI
	KRP 54	L	3	Krapina	Croatia	MPI	BD 11	R	3	Abri Bourgeois-Delaunay	France	MPI
	KRP 55	L	3	Krapina	Croatia	MPI	St-Césaire 1	R	4	Saint-Césaire	France	MPI
	KRP 59	L	4	Krapina	Croatia	MPI	Amud 1	R	4	Amud Cave	Israel	MPI
	BD 13	L	4	Abri Bourgeois-Delaunay	France	MPI	BD 15	L	4	Abri Bourgeois-Delaunay	France	MPI
	Regourdou 1	R	4	Regourdou	France	MPI	KRP D56	R	4	Krapina	Croatia	MPI
	St-Césaire 1	R	5	Saint-Césaire	France	MPI	KRP 50	R	5	Krapina	Croatia	MPI
							BD 16	R	5	Abri Bourgeois-Delaunay	France	MPI
NEA/EMH?	Tabun C2[c]	R	5	Tabun	Israel	MPI						
EMH	Dar es Soltane II H4	R	1	Dar es Soltane II Rabat	Morocco	MPI	Qafzeh 9	L	1	Qafzeh	Israel	MPI
	Qafzeh 9	L	1	Qafzeh	Israel	MPI	Qafzeh 15	R	1	Qafzeh	Israel	MPI
	Qafzeh 15	R	1	Qafzeh	Israel	MPI	Qafzeh 11	R	2	Qafzeh	Israel	MPI
	Qafzeh 26	R	2	Qafzeh	Israel	MPI	EQ-9	L	3	Equus Cave	South Africa	MPI
	Qafzeh 11	R	3	Qafzeh	Israel	MPI	Skhul IV	R	4	Skhul	Israel	MPI
	Qafzeh 8	R	4	Qafzeh	Israel	MPI						
	Skhul IV	R	4	Skhul	Israel	MPI						
UPMH	Nahal-Oren 14	R	1	Nahal Oren	Israel	MPI	Nahal-Oren 16	R	2	Nahal Oren	Israel	MPI
	Nahal-Oren 8	R	2	Nahal Oren	Israel	MPI	Nahal-Oren 24	R	2	Nahal Oren	Israel	MPI
	Hayonim 8	L	2	Hayonim	Israel	MPI	Hayonim 19	L	2	Hayonim	Israel	MPI
	Hayonim 19	L	2	Hayonim	Israel	MPI	Hayonim 25	R	3	Hayonim	Israel	MPI
	Hayonim 17	R	3	Hayonim	Israel	MPI	Hayonim 8	L	4	Hayonim	Israel	MPI
	Hayonim 20	L	3	Hayonim	Israel	MPI	Oberkassel D999	R	4	Bonn-Oberkassel	Germany	MPI
	Oberkassel D999	L	3	Bonn-Oberkassel	Germany	MPI						
MMH	Combe-Capelle	L	5	Combe-Capelle	France	MPI	Combe-Capelle	R	5	Combe-Capelle	France	MPI
RMH	Medieval $n = 17$		1-2: $n = 8$ 3. $n = 6$ 4: $n = 2$ 5: $n = 1$		Italy	CNR	Medieval $n = 11$		1-2: $n = 7$ 3: $n = 3$ 4: $n = 1$		Italy	CNR
	ULAC $n = 19$		1-2: $n = 13$ 3: $n = 5$ 4: $n = 1$		Various	MPI	Clinical $n = 11$		1-2: $n = 8$ 3: $n = 3$		Various	MPI

MicroCT data source: MPI (Max Planck Institute, Germany); ESRF (European Syncrotron Radiation Facility, France); CNR (Consiglio Nazionale delle Ricerche, Italy).
[a] Wear stages scored after Smith (1984).
[b] See Benazzi et al. (2014c).
[c] See Le Cabec et al. (2013).

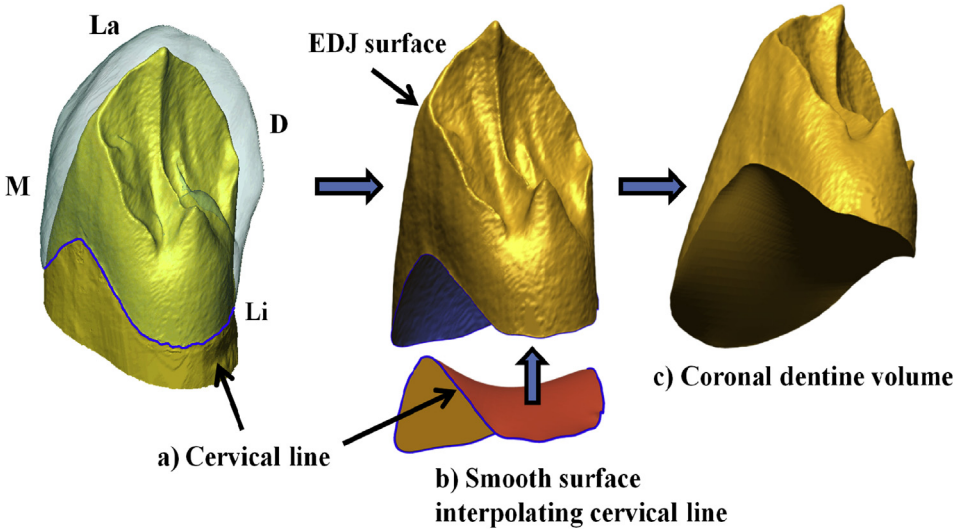

Figure 1. Illustration of the protocol (Benazzi et al., 2014a) used to isolate a standardized volume of coronal dentine in the Neandertal specimen Le Moustier 1 (lower right canine). a) A spline curve (blue) was digitized at the cemento-enamel junction which was then used to isolate the enamel–dentine junction (EDJ) surface. b) The cervical line was identified to interpolate a smooth non-planar surface from the uneven contour of the crown, thus c) closing the inferior surface of the coronal dentine core. M: mesial, Li: lingual, D: distal, La: labial. (For interpretation of the references to color in this figure legend, the reader is referred to the web version of this article.)

junction (EDJ) (S_{EDJ}, in mm^2). These values were subsequently used to compute the 3D average enamel thickness index (3D AET: V_{Enam}/S_{EDJ}, yielding the average straight-line distance (in mm) between the EDJ and the outer enamel surface, see Olejniczak et al., 2008c) and the 3D relative enamel thickness index (3D RET = 3D AET × $[V_{Dent}{}^{-1/3}]$ × 100, yielding a scale-free index suitable for intertaxon comparisons).

To discern differences in canine enamel thickness between Neandertal and all modern human groups (including early modern, Upper- and Epi-Paleolithic and recent modern humans), measurements for all components of enamel thickness and the resultant calculated 3D AET and 3D RET indices were tested in Past 3.11 (http://folk.uio.no/ohammer/past/; Hammer et al., 2001) using the Mann–Whitney U test ($\alpha = 0.05$; two-tailed) with a Monte Carlo permutation. The overall enamel thickness distribution was then computed in Avizo 7 as the minimum distance between the outer enamel surface and the underlying EDJ, and the results were displayed using a chromatic scale (from red to violet to represent thickest to thinnest enamel, respectively) of fixed range (from 0 to 1.3 mm with reference to the enamel thickness values observed in the sample), which allowed for the visual comparison of enamel thickness among all specimens.

The main results for the interspecific variation in both the 3D RET and 3D AET values were displayed as box plot charts using Past 3.11 (Figs. 2 and 3).

3. Results

Mean and standard deviation for V_{Enam}, V_{Dent}, S_{EDJ}, 3D AET and 3D RET indices for all specimens of lower and upper canines are reported in Tables 2 and 3, and in the Supplementary Online Material (SOM) Figures S1 and S2. Because of the relatively small UPMH sample size and the lack of significant differences between UPMH and RMH at wear stages 1–2 ($p > 0.05$), the results for UPMH are presented separately in Tables 2 and 3 but are combined with the RMH sample for statistical analysis. The significant *p*-values for statistical analysis are listed in Table 4. The debated Tabun C2 is not included in the statistical analysis, as for all other groups with a sample size smaller than four. The results for these individuals are shown in Tables 2 and 3, and are discussed separately.

3.1. Lower canines

Descriptive statistics for all enamel thickness variables and the 3D AET and 3D RET indices of lower canines are shown in Table 2. For wear stages 1–2, mean values for V_{Enam}, V_{Dent}, and S_{EDJ} in MH are significantly lower than those obtained for Neandertal and for EMH ($p < 0.001$), with EMH showing the highest V_{Enam} mean values. Even though 3D AET values do not differ between Neandertals and MH ($p = 0.7$), mean values for 3D RET (12.7 ± 1.6 and 15.5 ± 2.6, respectively) are significantly lower in Neandertals ($p = 0.0003$) (Fig. 2). For both 3D AET and 3D RET values, no significant differences were found between EMH and both Neandertals and MH ($p > 0.05$).

As would be expected, tooth wear was found to affect the values for all components of enamel thickness, especially V_{Enam}, ultimately affecting the 3D AET and 3D RET indices in all groups (Table 2). Of particular note, the results for the small sample of Neandertals with wear stages 3–4 must be treated with caution. At wear stage 3, the range of absolute and relative thickness variation between Neandertals and MH were similar, with the range of 3D AET values for Neandertals overlapping with the maximum values for MH and equivalent 3D RET between the two groups. Moreover, as shown in Figure 2 (e,f), no difference was found in the box-plots at wear stage 4 between Neandertals and MH for both 3D RET and 3D AET. On account of the small sample size, EMH at wear stage 3 (a single specimen) and single specimens for each taxa at wear stage 5 were excluded from any statistical analysis.

Among the different taxa (Table 2) Tabun C2 and the Mesolithic specimen from Combe-Capelle are classified at wear stage 5 where all taxa are represented by a single tooth. The Tabun C2 mandibular canine shows the lowest value for V_{Enam}, falling below the RMH range of distribution. Tabun C2 V_{Dent} is greater than MH, but close to NEA, while its S_{EDJ} falls close to Combe-Capelle. Moreover, the 3D AET in Tabun C2 (0.52 mm) is close to the RMH (0.54 mm), while its 3D RET value (10.3) is slightly smaller than in RMH (11.3). Finally, the V_{Enam} of Combe-Capelle is higher than the NEA value, the V_{Dent} is close to the RMH value, and both its 3D AET (0.7 mm) and 3D RET (14.2) values fall slightly above the NEA values (0.6 mm and 12.03, respectively).

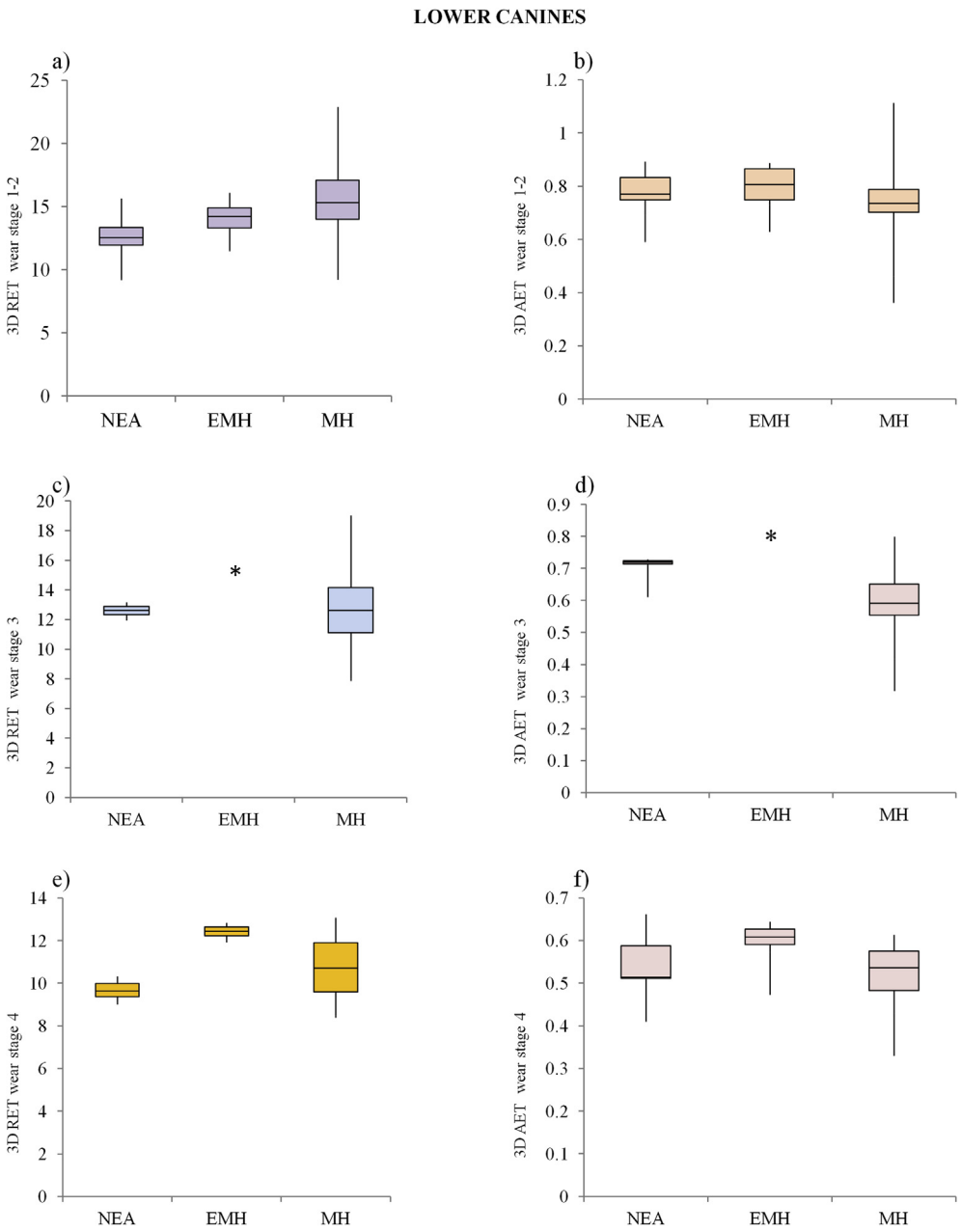

Figure 2. 3D relative enamel thickness (3D RET) and average enamel thickness (3D AET, mm) box plots (standard deviation interquartile method) for lower canines at wear stages 1–2 (a; b), 3 (c; d) and 4 (e; f) for Neandertals (NEA), early modern humans (EMH) and modern humans (MH). Single individuals are represented by an asterisk (*).

As shown in Figure 4, both NEA and MH lower canines present thicker labial enamel (involving both distal and mesial marginal ridges) in the cuspal half of the crown than in the cervical half of the crown. As further shown in the lingual views (Fig. 4), the enamel cap is thicker on the distal aspect of the crowns than on the mesial aspect. Although this pattern is recognizable in both NEA and MH, the labial enamel is noticeably thicker on the incisal half of the MH canines. Importantly, the mesial and distal marginal ridges, which form the typical shovel-shaped morphology in the lingual aspect of Neandertal lower canines, are not associated with enamel thickening; in other words, the enamel follows the profile of the dentine.

3.2. Upper canines

Descriptive statistics for all enamel thickness variables and for the 3D AET and 3D RET indices for upper canines are shown in Table 3. At wear stages 1–2, Neandertals have significantly higher V_{Enam}, V_{Dent} and S_{EDJ} values than MH ($p < 0.001$). The two groups do not differ in 3D AET ($p = 0.6$), but Neandertals have significantly lower 3D RET values than MH ($p = 0.03$). In EMH, both 3D AET and 3D RET are greater than in MH, mainly due to a greater enamel volume (statistically similar to that of Neandertals) combined with a reduced EDJ surface area (statistically similar to that of MH). The mean value of 3D AET for EMH (1.27 ± 0.4 mm) is not far from that of Neandertals (0.9 ± 0.09 mm; $p = 0.09$) but is significantly greater than MH (0.88 ± 0.1 mm; $p = 0.017$). Furthermore, the 3D RET

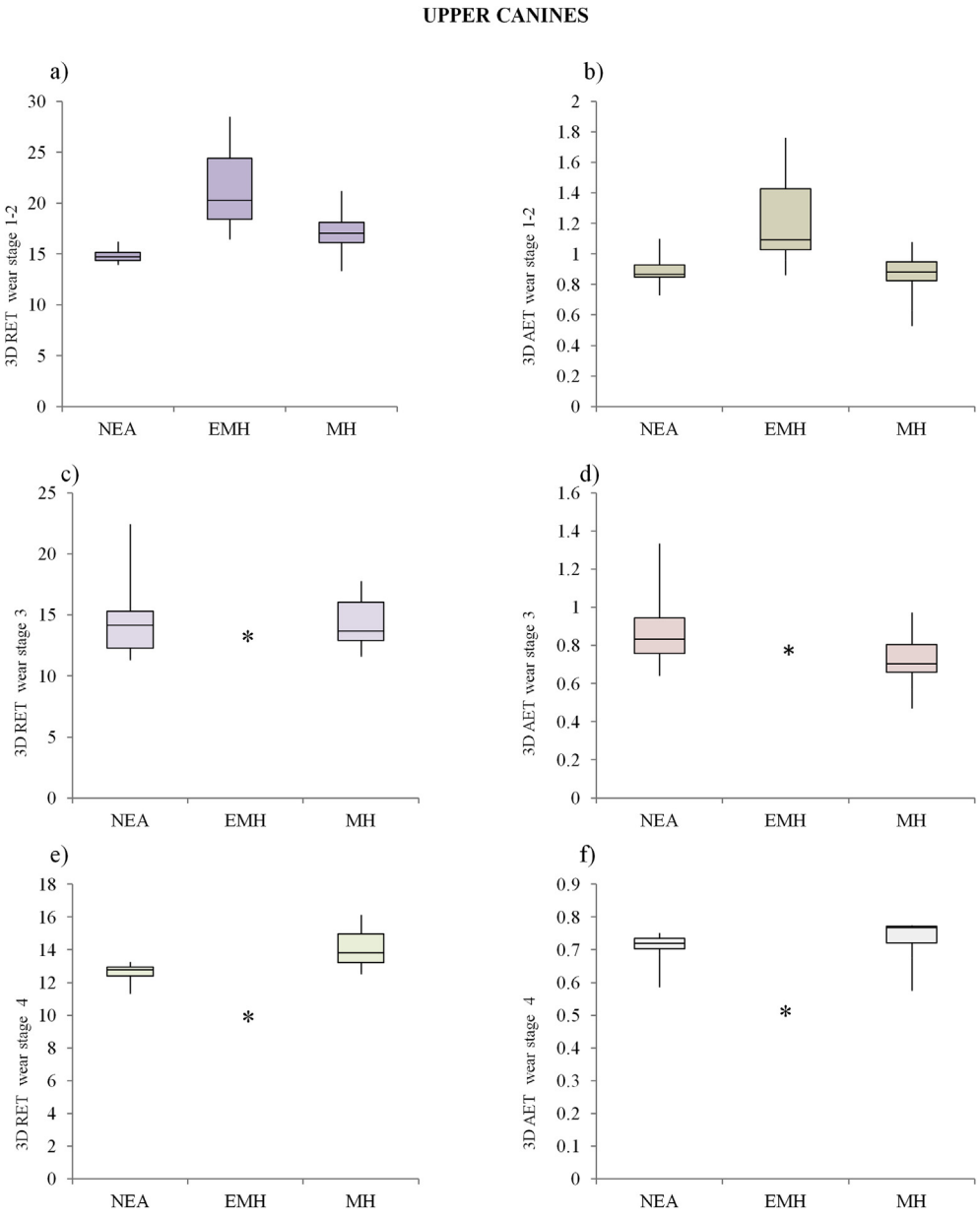

Figure 3. 3D relative enamel thickness (3D RET) and average enamel thickness (3D AET, mm) box plots (standard deviation interquartile method) for upper canines at wear stages 1–2 (a; b), 3 (c; d) and 4 (e; f) for Neandertal (NEA), early modern humans (EMH) and modern humans (MH). Single individuals are represented by an asterisk (*).

values of EMH are significantly higher than MH ($p = 0.02$) and Neandertals ($p = 0.017$; Fig. 3a).

As observed for the lower canines, tooth wear affects crown measurements (mainly enamel volume), ultimately influencing the calculated 3D AET and 3D RET values. Neandertals and MH teeth at wear stage 3 were found to significantly differ in enamel volume ($p < 0.05$); however, they do not differ in either 3D AET ($p = 0.07$) or 3D RET ($p = 0.7$) (Fig. 3c,d). Similarly, at wear stage 4 the range of variation in 3D AET and 3D RET values for Neandertals and MH do not differ (Fig. 3e,f).

Finally, Combe-Capelle (wear stage 5) could be compared with only two Neandertals, and all of its enamel thickness components fall clearly below the mean for Neandertals. By contrast, both 3D AET (0.7 mm) and 3D RET (14.1) fall within the range of variation of Neandertals.

The pattern of enamel distribution observed in the upper canines of Neandertals and modern humans is consistent with that described above for lower canines (Fig. 4): the enamel is thicker on the labial aspect of the crown, specifically in the incisal half, involving both distal and mesial marginal ridges. The labial region of the crown is visibly thicker in the upper canines compared to the lowers, as reflected in the color map. Moreover, in contrast to the lower canines, a tendency was observed for MH to have thicker enamel in the incisal half of the lingual aspect of the crown. Overall, for both Neandertals and MH, upper canines have significantly greater 3D AET and 3D RET values than the lower canines (NEA: $p = 0.005$ and $p = 0.02$, respectively; MH: $p < 0.001$ and $p = 0.04$, respectively).

4. Discussion and conclusions

4.1. Taxonomic discrimination

Studies of molar teeth have revealed that Neandertals and modern humans differ in their enamel thickness distribution

Table 2
Descriptive statistics for the volume of enamel (V_{Enam}, mm^3), volume of the dentine and the pulp cavity in the crown (V_{Dent}, mm^3), the enamel–dentine junction surface area (S_{EDJ}, mm^2), 3D average enamel thickness (3D AET, in mm) and 3D relative enamel thickness (3D RET, scale-free index) of the lower canines of the study sample are reported. SD: standard deviation.

Taxon	*n*	Wear stage	V_{Enam}	V_{Dent}	S_{EDJ}	3D AET	3D RET
			Mean (SD)	Mean (SD)	Mean (SD)	Mean (SD)	Mean (SD)
NEA	11	1–2	135.8 (43)	235.1 (100.6)	175.7 (42.4)	0.76 (0.07)	12.7 (1.6)
EMH	4	1–2	143.4 (33.5)	197.9 (49.0)	179 (47.9)	0.82 (0.08)	14.01 (1.9)
UPMH	4	1–2	87.2 (7.6)	115.4 (19)	116.4 (8.1)	0.75 (0.11)	15.6 (3)
RMH	21	1–2	89.02 (18.3)	116.6 (25.3)	119.5 (21.1)	0.75 (0.12)	15.5 (2.6)
MH	25	1–2	88.7 (16.9)	116.5 (24.1)	119 (19.5)	0.75 (0.12)	15.5 (2.6)
NEA	2	3	114 (8.1)	186.8 (24.7)	158.6 (14)	0.71 (0.1)	12.6 (0.8)
EMH	1	3	110.7	148.4	135.8	0.81	15.4
UPMH	3	3	61.3 (7.2)	103.6 (22.5)	104.4 (17.8)	0.59 (0.44)	12.8 (2.0)
RMH	11	3	65.9 (12.1)	110.7 (25.6)	113.7 (24.4)	0.61 (0.1)	12.80 (3)
MH	14	3	66.9 (11.4)	110.8 (24.4)	112.7 (22.9)	0.60 (0.1)	12.8 (2.7)
NEA	3	4	78 (20.8)	197.06 (59.5)	137.48 (15.5)	0.56 (0.09)	9.7 (0.61)
EMH	2	4	60.8 (7.7)	117.3 (13.1)	99.7 (4.3)	0.61 (0.05)	12.4 (0.6)
RMH	3	4	57.8 (6.7)	119.6 (14.1)	111.0 (13.7)	0.53 (0.09)	10.8 (2.3)
NEA	1	5	61.1	126	101.4	0.6	12.03
Tabun C2	1	5	47.3	127.5	91.06	0.52	10.3
MMH	1	5	64.23	116.4	92.6	0.7	14.2
RMH	1	5	58.2	112.7	106.9	0.54	11.3

NEA = Neandertal; UPMH = Upper Paleolithic modern human; MMH = Mesolithic modern human; RMH = recent modern human; MH = modern human (UPMH + RMH); EMH = early modern human.

Table 3
Descriptive statistics for the volume of enamel (V_{Enam}, mm^3), volume of the dentine and pulp cavity in the crown (V_{Dent}, mm^3), the enamel -dentine junction surface area (S_{EDJ}, mm^2), 3D average enamel thickness (3D AET, in mm) and 3D relative enamel thickness (3D RET, scale-free index) of the upper canines of the study sample. SD: standard deviation.

Taxon	*n*	Wear stage	V_{Enam}	V_{Dent}	S_{EDJ}	3D AET	3D RET
			Mean (SD)	Mean (SD)	Mean (SD)	Mean (SD)	Mean (SD)
NEA	6	1–2	154.4 (26.7)	231.5 (42)	176.9 (12.3)	0.9 (0.09)	14.9 (0.8)
EMH	3	1–2	172.4 (32.4)	196.5 (39.9)	140 (21.7)	1.27 (0.4)	21.8 (6.1)
UPMH	3	1–2	119.25 (10.8)	159.6 (15.7)	131.5 (4.2)	0.91 (0.11)	16.8 (2.1)
RMH	15	1–2	110.86 (25.2)	137.9 (28.7)	126.6 (18.2)	0.87 (0.11)	17.1 (2.1)
MH	18	1–2	112.34 (23.5)	141.8 (28.2)	127.5 (16.8)	0.88 (0.11)	17.0 (2.1)
NEA	6	3	149.2 (22.2)	232.3 (40.8)	169 (33.2)	0.91 (0.2)	14.9 (4.02)
EMH	1	3	103.4	186.3	135.9	0.76	13.3
UPMH	1	3	128.2	163.7	131.7	0.97	17.8
RMH	6	3	89.22 (17.2)	129.6 (24.5)	127.71 (17.1)	0.70 (0.1)	13.9 (1.8)
MH	7	3	94.79 (21.6)	134.5 (25.8)	128.28 (15.7)	0.74 (0.14)	14.4 (2.2)
NEA	4	4	103.1 (4.6)	189.0 (19.0)	143.6 (10.04)	0.72 (0.03)	12.6 (0.8)
EMH	1	4	77.1	129.2	149.9	0.52	10.2
UPMH	2	4	90.0 (22.6)	142.3 (49)	116.6 (28.41)	0.77 (0.01)	15 (1.6)
RMH	1	4	87.5	152.75	129.7	0.68	12.62
MH	3	4	89.2 (16.1)	145.8 (35.16)	121 (21.47)	0.7 (0.06)	14.2 (1.8)
NEA	2	5	104.7 (17.9)	196.8 (13.9)	143.08 (4.9)	0.7	12.7 (2.9)
MMH[a]	1	5	55	110	81	0.7	14.1

NEA = Neandertal; UPMH = Upper Paleolithic modern human; MMH = Mesolithic modern human; RMH = recent modern human; MH = modern human (UPMH + RMH); EMH = early modern human.
[a] Combe-Capelle.

Table 4
Results of the Mann–Whitney U test ($\alpha = 0.05$; two-tailed) and the Monte Carlo permutation obtained from the crown components comparison for the canines study sample groups.[b] Significant *p*-values in bold.

	Taxa	Wear stage[a]	V_{Enam}	V_{Dent}	S_{EDJ}	3D AET	3D RET
			p	p	p	p	p
Lower canines	RMH/UPMH	1–2	0.9	0.97	0.86	0.97	0.91
	EMH/MH	1–2	**0.002**	**0.0004**	**0.001**	0.26	0.3
	NEA/MH	1–2	**0.0001**	**0.0001**	**0.0001**	0.7	**0.0003**
	NEA/EMH	1–2	0.67	0.75	0.85	0.41	0.3
Upper canines	RMH/UPMH	1–2	0.49	0.07	0.2	0.7	1
	EMH/MH	1–2	**0.006**	**0.015**	0.3	**0.017**	**0.02**
	NEA/MH	1–2	**0.0001**	**0.0002**	**0.0001**	0.6	**0.03**
	NEA/EMH	1–2	0.7	0.4	**0.05**	0.09	**0.02**
	NEA/MH	3	**0.005**	**0.0007**	**0.035**	0.07	0.7

NEA = Neandertal; UPMH = Upper Paleolithic modern human; MMH = Mesolithic modern human; RMH = recent modern human; MH = modern human (UPMH + RMH); EMH = early modern human.
[a] Based on Smith (1984).
[b] The groups listed in the table are sample size >4 individuals.

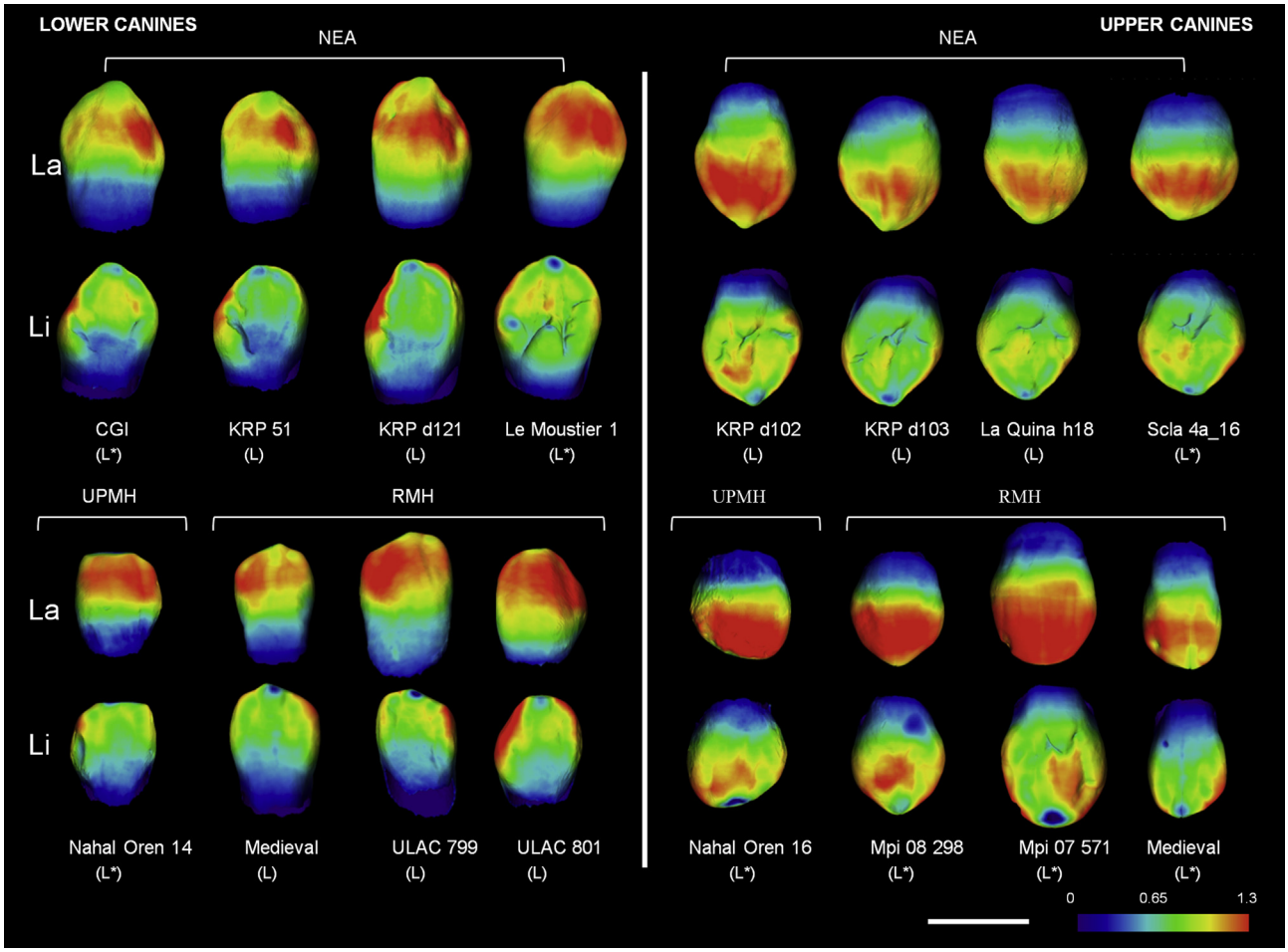

Figure 4. 3D enamel thickness distribution maps in a subsample of Neandertal and modern human lower and upper canines (wear stages 1–2) visualized using spectral colors. While the thickest enamel is represented in red, the thinnest enamel appears in violet (see color-scale with the corresponding enamel thickness in mm). La = labial, Li = lingual. L = left; R = right. White scale bar = 1 cm. Color scale: 0–1.3 cm. All the teeth are represented as left canines; right canines have been mirrored and marked in the image as (L*). (For interpretation of the references to color in this figure legend, the reader is referred to the web version of this article.)

(Macchiarelli et al., 2006; Olejniczak et al., 2008a). Although both groups possess a similar volume of enamel, this volume is deposited over a more complex EDJ and is associated with a higher volume of dentine and a larger EDJ surface area in Neandertals. This relationship ultimately leads to a slightly lower 3D AET and significantly lower 3D RET compared to modern humans (Smith et al., 2007; Bayle et al., 2009a). This finding was confirmed using both 2D approaches (e.g., Smith et al., 2012; Fornai et al., 2014) and advanced 3D methods utilizing the entire enamel cap and associated underlying crown dentine (Olejniczak et al., 2008a; Bayle et al., 2009b).

By contrast, few researchers have included the anterior dentition in their analyses. Bayle et al. (2009a) reported volumetric values and dental tissue proportions of the lower deciduous dentition, including the anterior teeth, in the Roc-de-Marsal Neandertal child and in a modern human specimen. Despite the small sample size (two specimens), the authors observed that the anterior teeth of Roc-de-Marsal have lower 2D RET values than the modern human specimen. Benazzi et al. (2015a) analyzed deciduous lower lateral incisors, confirming significant differences in the 3D components of enamel thickness between Neandertals and modern humans. As concerns the permanent anterior dentition, only one study (Smith et al., 2012) has investigated 2D enamel thickness variation in canine teeth in a sample of fossil and extant teeth belonging to taxa within the genus *Homo*. The authors used digital cross-sections to show that Neandertal canines have lower 2D AET and RET values due to markedly greater dentine areas and EDJ lengths than in modern humans, including both fossil and recent modern specimens. As enamel thickness distribution is not homogeneously distributed in the crown, it is important to emphasize that a 2D section of the tooth (physical or digital) cannot account for the entire 3D morphological complexity of the crown.

Our results confirm previous findings (Benazzi et al., 2014a) and demonstrate that both lower and upper canines of Neandertals provide significantly lower 3D RET values than modern humans, while 3D AET is not distinctive for interspecific analysis, even considering that Neandertals have significantly higher enamel volume than MH, contrary to the similar volume of enamel observed for molars.

Despite this, the 3D AET index has been found to differ significantly between upper and lower canines at wear stage 1–2 for both Neandertals and modern humans ($p = 0.0072$ and $p = 0.002$ respectively), suggesting that upper and lower canines can not be pooled for statistical analysis.

The greater EDJ surface area in the Neandertal canines reflects their more complex morphology, namely a generally more pronounced mesial and distal marginal ridge and a bulbous lingual tubercle and median ridge (Fig. 5). This is associated with a greater absolute volume

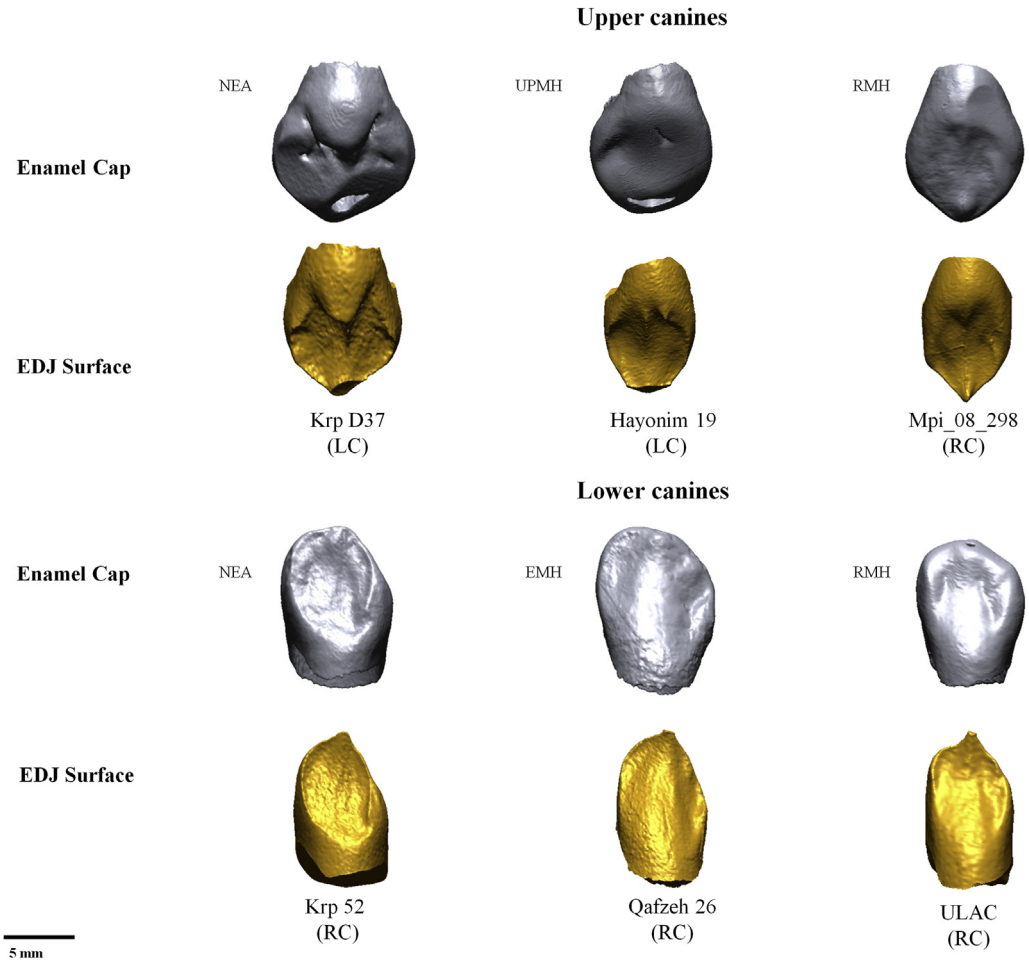

Figure 5. 3D models of the enamel cap (in gray) and of the EDJ surface (in gold) in upper and lower permanent canines of Neandertal (NEA), early modern humans (EMH), UPMH (Upper- and Epi-Paleolithic modern humans) and recent modern humans (RMH). RC = right canine; LC = left canine. (For interpretation of the references to color in this figure legend, the reader is referred to the web version of this article.)

of the dentine core in Neandertals compared to modern humans, which accounts for the lower 3D RET values in the former.

Preliminary results based on only three early modern human specimens may suggest that their lower canines are within the range of variation of Neandertals for all individual crown components of enamel thickness, yet with significantly greater 3D AET values than NEA and MH but with an intermediate position between Neandertals and modern humans for 3D RET. By contrast, although the EMH upper canines are in the range of variation of Neandertals for enamel and dentine volumes, this is not the case for the EDJ surface area and the 3D RET values. Contrary to modern populations, EMH have a smaller enamel volume than MH but a similar S_{EDJ} which ultimately contributes to their relatively thicker enamel. However, these results should be treated with caution on account of the small size of the EMH sample.

The general pattern of interspecific differences between Neandertals and MH is observed in both upper and lower canines for the components of enamel thickness described above. Moreover, the upper canines of both Neandertals and MH are characterized by greater 3D AET and 3D RET than the lower canines.

Overall, our results confirm that the 3D RET index is a valuable parameter to discriminate between Neandertals and Upper Paleolithic/recent modern human canines which are unworn or slightly worn (wear stages 1–2). In particular, because of the relationship with other factors, such as sexual dimorphism in this tooth class (Feeney et al., 2010), we do not rely on single measurements to assess the inter-taxa variability. In fact, V_{Enam}, V_{DENT}, and S_{EDJ} are considered to be the result of average values and indices that do not account for sexual variability. Ultimately, the index reliably accounts for the inter-variability. Furthermore, the results have effectively been shown to discriminate between Neandertal and MH, despite any possible internal variation due to sex or population differences.

The discriminatory power of the 3D RET index appears to decrease with tooth wear, particularly for the upper canines at wear stage 3 for which a sample suitable for statistical analysis was available. This result is corroborated by visual examination of the enamel thickness color map (Fig. 4). The shoulders and cuspal half of the labial aspect of the crown are relatively thicker than the remainder of the crown in both Neanderthals and in modern humans in particular. This region of the crown is already affected at early wear stages, and this loss of enamel affects the calculated 3D AET and 3D RET indices. It is therefore logical to assume that this then affects the taxonomic differences between the two groups. In spite of this, as worn teeth are more frequently found in the fossil record than unworn teeth, efforts to explore the discriminatory power of worn teeth, including (but not limited to) enamel thickness, would assist in dental analyses as suggested by other authors (Fornai et al., 2014; Benazzi et al., 2015a).

In conclusion, the general pattern of enamel thickness distribution (i.e., enamel thickening on the incisal half of the labial aspect of the crown and reduced enamel on the lingual aspect), is similar among Neandertal and modern human canines, with the 3D RET index providing a useful tool to discriminate unworn or slightly worn teeth. Based on the sample studied here, it is clear that heavy wear affecting the incisal part of the canine crown impedes the use of the RET index in 3D for discriminating Neandertals from modern humans.

4.2. Functional implications of enamel distribution

It is unclear whether interspecific (Neandertals versus modern humans) and/or intraspecific (lower versus upper canines) differences observed here for lower and upper canines have functional implications and/or whether they represent the result of random events, as suggested for other dental features, including taurodontism. Recent studies on taurodontism (a morphological variant frequently observed in Neandertal molar teeth and characterized by an enlargement of the pulp chamber with apical displacement of the root bifurcation; Bailey, 2002), revealed that this trait does not improve dental biomechanics and may be instead an adaptation to a high attrition diet or even the result of pleiotropic or genetic drift events (Benazzi et al., 2015b).

Interestingly, our results show that Neandertals have greater enamel volume than modern humans, in contrast to the similar volume of enamel observed for molars in both taxa. This result sheds light on the difference in enamel volume between canines and molars, maybe due to different paramasticatory activities (see Le Cabec et al., 2013 for a review) or differences in molecular signaling for the enamel knots in the single cusped canine (Jernvall and Thesleff, 2000, 2012; Thesleff et al., 2001) which requires further investigation.

As far as enamel thickness is concerned, several studies suggest that, in comparison with modern humans, Neandertal molars (and anterior teeth to a certain extent) may be characterized by thinner enamel, faster crown extension rates and a shorter crown formation (Ramirez Rozzi and Bermudez de Castro, 2004; Bayle et al., 2009a,b; Smith et al., 2010). Differences in the relation between anterior and posterior teeth in both absolute and relative crown size between Neandertals and modern humans (Smith et al., 2007) might play an important role in this debate. At present, however, it is not possible to validate an interpretative model specifically relating dental maturational pattern to tooth size (Bayle et al., 2009a).

Therefore, as far as the canines are concerned, it might be that functional, ontogenetic factors and genetic drift effects, or some combination of these, are involved. It is reasonable to assume that the general pattern of enamel thickness distribution (i.e., enamel thickening on the incisal half of the labial aspect of the crown and reduced enamel on the lingual aspect), similar in Neandertal and modern human canines, has some biomechanical advantages for withstanding labiolingual bending forces acting on the tooth, and ultimately resulting in high tensile stresses labially and more compressive stresses lingually (Kupczik and Chattah, 2014). It has been demonstrated that tension is more damaging to enamel than compression (e.g., Gillings and Buonocore, 1961; Dejak et al., 2005; Benazzi et al., 2011) and therefore it might be that greater enamel thickness on the labial aspect contributes to reducing enamel fractures. At the same time, we cannot rule out the hypothesis that greater dentine volume in Neandertals is an additional feature to improve dental biomechanics, i.e., for withstanding and distributing the occlusal loading (Le Cabec et al., 2012, 2013). Moreover, it is reasonable to assume that the enamel distribution reflects the macrowear pattern of the canines, as suggested by Le Luyer et al. (2014), whose results revealed a correlation between molar wear pattern and enamel thickness associated with dietary changes, with relatively thicker enamel possibly evolving as a plastic response to withstand wear.

Our results demonstrated that, in both Neandertals and modern humans, the mesial and particularly the distal shoulders of the crown are thickly enameled in the areas where wear facets develop. Future research is needed to evaluate whether biomechanical advantages or an adaptation to a high attrition diet were driving the selection for the dental tissue crown components and resultant pattern of enamel distribution in the canines. Biomechanical approaches, ideally finite element methods, would help clarify whether functional aspects, pleiotropic effects, or genetic drift are responsible for the enamel thickness patterns described here (Benazzi et al., 2013a,b, 2015b; Kupczik and Chattah, 2014).

Acknowledgments

We are grateful to the curators and collaborators who granted access to the dental material: B. Arensburg, S.E. Bailey, A. Barash, O. Bar-Yosef, E. Been, A. Ben-n'cer, D. Bonjean, the City of Andenne (Belgium) and Archéologie Andennaise, P. Brown, J.-J. Cleyet-Merle, A.P. Derevianko, M.A. El Hajraoui, I. Fawzi, C. Feja, U.A. Glasmacher, F. E. Grine, F. Gröning, M. Hänel, I. Hershkovitz, A. Hoffmann, O. Kullmer, S. Markin, P. Mennecier, V. Merlin-Langlade, NESPOS, S. Pääbo, P. Périn, J. Radovčić, Y. Rak, S. Raoui, J.-P. Raynal, D. Reid, A. Rosas, A. Savariego, R. Schmitz, F. Schrenk, C. Schwab, P. Semal, T.M. Smith, M.V. Shunkov, A. Soficaru, F. Spoor, J.-F. Tournepiche, M. Toussaint, B. Vandermeersch, C. Verna, B. Viola and R. Ziegler. We thank A. Winzer, P. Schönfeld, H. Temming, T. Smith and M. Skinner for their micro-CT scanning expertise at MPI-EVA, and R. Tilgner and D. Plotzki for technical assistance. We thank the staff of the ID19 beamline at the ESRF for technical expertise and granting access to the synchrotron data. We are additionally grateful to J. Michael Plavcan (Editor), to the Associate Editor and to the three anonymous reviewers for their insightful comments which considerably improved the quality of this manuscript. This research was funded by the Max Planck Society and the European Research Council (ERC) under the European Union's Horizon 2020 research and innovation program (grant agreement n. 724046 – SUCCESS); www.erc-success.eu.

Supplementary Online Material

Supplementary online material related to this article can be found at http://dx.doi.org/10.1016/j.jhevol.2017.08.009.

References

Bailey, S.E., 2002. A closer look at Neanderthal postcanine dental morphology: the mandibular dentition. Anat. Rec. 269, 99–106.

Bayle, P., Dean, M.C., 2013. New way to think about enamel and dentine thickness in longitudinal tooth sections. In: Proceedings of the 15th International Symposium on Dental Morphology, Newcastle upon Tyne, UK, 2011. Bull. Int. Assoc. Paleodont., vol. 7, pp. 29–37.

Bayle, P., Braga, J., Mazurier, A., Macchiarelli, R., 2009a. Dental developmental pattern of the Neanderthal child from Roc-de-Marsal: a high-resolution 3D analysis. J. Hum. Evol. 56, 66–75.

Bayle, P., Braga, J., Mazurier, A., Macchiarelli, R., 2009b. Brief communication: high-resolution assessment of the dental developmental pattern and characterization of tooth tissue proportions in the late Upper Paleolithic child From La Madeleine, France. Am. J. Phys. Anthropol. 138, 493–498.

Bayle, P., Macchiarelli, R., Trinkaus, E., Duarte, C., Mazurier, A., Zilhão, J., 2010. Dental maturational sequence and dental tissue proportions in the early Upper Paleolithic child from Abrigo do Lagar Velho, Portugal. PNAS 107, 1338–1342.

Bayle, P., Alcaraz, M., Zapata, J., Lombardi, V.A., Pérez-Pérez, A., Pinilla, B., Le Luyer, M., Robson Brown, K.A., Romero, A., Willman, J.-C., Lacy, S.A., Ortega, J., Karaková, K., 2017. The Palomas dental remains: enemal thickness and tissues proportions. In: Trinkaus, E., Walker, M.J. (Eds.), The people of Palomas: neandertals from the Sima de las Palomas del Cabezo Gordo, Southeastern Spain (Texas A&M University Anthropology Series), pp. 115–137. College Station, Texas.

Benazzi, S., Kullmer, O., Grosse, I.R., Weber, G.W., 2011. Using occlusal wear information and finite element analysis to investigate stress distributions in human molars. J. Anat. 219, 259–272.
Benazzi, S., Nguyen, H.N., Kullmer, O., Hublin, J.J., 2013a. Unravelling the functional biomechanics of dental features and tooth wear. PLOS ONE 8, e69990. http://dx.doi.org/10.1371/journal.pone.0069990.
Benazzi, S., Nguyen, H.N., Schulz, D., Grosse, I.R., Gruppioni, G., Hublin, J.J., Kullmer, O., 2013b. The evolutionary paradox of tooth wear: simply destruction or inevitable adaptation? PLOS ONE 8, e62263. http://dx.doi.org/10.1371/journal.pone.0062263.
Benazzi, S., Panetta, D., Fornai, C., Toussaint, M., Gruppioni, G., Hublin, J.J., 2014a. Technical Note: Guidelines for the digital computation of 2D and 3D enamel thickness in hominoid teeth. Am. J. Phys. Anthropol. 153, 305–313.
Benazzi, S., Bailey, S.E., Peresani, M., Mannino, M.A., Romandini, M., Richards, M.P., Hublin, J.J., 2014b. Middle Paleolithic and Uluzzian human remains from Fumane Cave. Italy. J. Hum. Evol. 70, 61–68.
Benazzi, S., Toussaint, M., Hublin, J.J., 2014c. Enamel thickness in the Scladina 1-4A Neandertal teeth. In: Toussaint, M., Bonjean, D. (Eds.), The Scladina 1-4A Juvenile Neandertal (Andenne, Belgium): Palaeoanthropology and Context, vol. 134. ERAUL, pp. 307–314.
Benazzi, S., Slon, V., Talamo, S., Negrino, F., Peresani, M., Bailey, S.E., Sawyer, S., Panetta, D., Vicino, G., Starnini, E., Mannino, M.A., Salvadori, P.A., Meyer, M., Pääbo, S., Hublin, J.-J., 2015a. The makers of the Protoaurignacian and implications for Neandertal extinction. Sci. Rep. 348, 793–796.
Benazzi, S., Nguyen, H.N., Kullmer, O., Hublin, J.J., 2015b. Exploring the biomechanics of taurodontism. J. Anat. 226, 180–188.
Clement, A.F., Hillson, S.W., Aiello, L.C., 2012. Tooth wear, Neanderthal facial morphology and the anterior dental loading hypothesis. J. Hum. Evol. 62, 367–376.
Crevecoeur, I., Bayle, P., Rougier, H., Maureille, B., Higham, T., van der Plicht, J., de Clerck, N., Semal, P., 2010. The Spy VI child: A newly discovered Neandertal infant. J. Hum. Evol. 59, 641–656.
Dejak, B., Młotkowski, A., Romanowicz, M., 2005. Finite element analysis of mechanism of cervical lesion formation in simulated molars during mastication and parafunction. J. Prosth. Dent. 94, 520–529.
Feeney, R.N.M., Zermeno, J.P., Reid, D.J., Nakashima, S., Sano, H., Bahar, A., Hublin, J.-J., Smith, T.M., 2010. Enamel thickness in Asian human canines and premolars. Anthropol. Sci. 118, 191–198.
Feldkamp, L.A., Davis, L.C., Kress, J.W., 1984. Practical cone-beam algorithm. J. Opt. Soc. Am. A 1, 612–619.
Fornai, C., Benazzi, S., Svoboda, J., Pap, I., Harvati, K., Weber, G.W., 2014. Enamel thickness variation of deciduous first and second upper molars in modern humans and Neanderthals. J. Hum. Evol. 76, 83–91.
Gillings, B., Buonocore, M., 1961. An investigation of enamel thickness in human lower incisor teeth. J. Dent. Res. 40, 105–118.
Grine, F.E., 2002. Scaling of tooth enamel thickness, and molar crown size reduction in modern humans. S. Afr. J. Sci. 98, 503–509.
Grine, F.E., 2005. Enamel thickness of deciduous and permanent molars in modern *Homo sapiens*. Am. J. Phys. Anthropol. 126, 14–31.
Grine, F.E., Klein, R.G., 1985. Pleistocene and Holocene human remains from Equus Cave, South Africa. Anthropology 8, 55–98.
Grine, F.E., Spencer, M.A., Demes, B., Smith, H.F., Strait, D.S., Constant, D.A., 2005. Molar enamel thickness in the chacma baboon, *Papio ursinus* (Kerr 1792). Am. J. Phys. Anthropol. 128, 812–822.
Hammer, Ø., Harper, D.A.T., Ryan, P.D., 2001. Paleontological statistics software package for education and data analysis. Palaeontol. Electron. 4, 9–18.
Hauser, O., 1924. Der Mensch vor 100.000 Jahren. Jena.
Hoffmann, A., Hublin, J.-J., Hüls, M., Terberger, T., 2011. The *Homo aurignaciensis hauseri* from Combe-Capelle – a Mesolithic burial. J. Hum. Evol. 61, 211–214.
Jernvall, J., Thesleff, I., 2000. Reiterative signaling and patterning during mammalian tooth morphogenesis. Mech. Dev. 92, 19–29.
Jernvall, J., Thesleff, I., 2012. Tooth shape formation and tooth renewal: evolving with the same signals. Development 139, 3487.
Kono, R.T., 2004. Molar enamel thickness and distribution patterns in extant great apes and humans: new insights based on a 3-dimensional whole crown perspective. Anthropol. Sci. 112, 121–146.
Kono, R.T., Suwa, G., 2008. Enamel distribution patterns of extant human and hominoid molars: occlusal versus lateral enamel thickness. Bull. Natl. Mus. Nat. Sci. D 34, 1–9.
Kono, R.T., Suwa, G., Tanijiri, T., 2002. A three-dimensional analysis of enamel distribution patterns in human permanent first molars. Arch. Oral Biol. 47, 867–875.
Kupczik, K., Chattah, N.L.T., 2014. The adaptive significance of enamel loss in the mandibular incisors of cercopithecine primates (mammalia: Cercopithecidae): A finite element modelling study. PLOS ONE 9, e97677. http://dx.doi.org/10.1371/journal.pone.0097677.
Le Cabec, A., Kupczik, K., Gunz, P., Braga, J., Hublin, J.J., 2012. Long anterior mandibular tooth roots in Neanderthals are not the result of their large jaws. J. Hum. Evol. 63, 667–681.
Le Cabec, A., Gunz, P., Kupczik, K., Braga, J., Hublin, J.J., 2013. Anterior tooth root morphology and size in Neanderthals: Taxonomic and functional implications. J. Hum. Evol. 64, 169–193.
Le Luyer, M., Rottier, S., Bayle, P., 2014. Brief communication: Comparative patterns of enamel thickness topography and oblique molar wear in two early Neolithic and Medieval population samples. Am. J. Phys. Anthropol. 155, 162–172.
Macchiarelli, R., Bondioli, L., Debenath, A., Mazurier, A., Tournepiche, J.F., Birch, W., Dean, M.C., 2006. How Neanderthal molar teeth grew. Nature 444, 748–751.
Martin, L., 1985. Significance of enamel thickness in hominoid evolution. Nature 314, 260–263.
Martin, L.B., 1983. The relationships of the later Miocene Hominoidea. Ph.D. Dissertation, University College London.
Martin, L.B., Olejniczak, A.J., Maas, M.C., 2003. Enamel thickness and microstructure in pitheciin primates, with comments on dietary adaptations of the middle Miocene hominoid *Kenyapithecus*. J. Hum. Evol. 45, 351–367.
Molnar, S., Gantt, D.G., 1977. Functional implications of primate enamel thickness. Am. J. Phys. Anthropol. 46, 447–454.
Olejniczak, A.J., Grine, F.E., 2006. Assessment of the accuracy of dental enamel thickness measurements using microfocal X-ray computed tomography. Anat. Rec. A Discov. Mol. Cell. Evol. Biol. 288, 263–275.
Olejniczak, A.J., Gilbert, C.C., Martin, L.B., Smith, T.M., Ulhaas, L., Grine, F.E., 2007. Morphology of the enamel-dentine junction in sections of anthropoid primate maxillary molars. J. Hum. Evol. 53, 292–301.
Olejniczak, A.J., Smith, T.M., Skinner, M.M., Grine, F.E., Feeney, R.N.M., Thackeray, J.F., Hublin, J.-J., 2008a. Three-dimensional molar enamel distribution and thickness in *Australopithecus* and *Paranthropus*. Biol. Lett. 4, 406–410.
Olejniczak, A.J., Tafforeau, P., Feeney, R.N.M., Martin, L.B., 2008b. Three-dimensional primate molar enamel thickness. J. Hum. Evol. 54, 187–195.
Olejniczak, A.J., Smith, T.M., Feeney, R.N.M., Macchiarelli, R., Mazurier, A., Bondioli, L., Rosas, A., Fortea, J., de la Rasilla, M., Garcia-Tabernero, A., Radovčic, J., Skinner, M.M., Toussaint, M., Hublin, J.J., 2008c. Dental tissue proportions and enamel thickness in Neandertal and modern human molars. J. Hum. Evol. 55, 12–23.
Panetta, D., Belcari, N., Del Guerra, A., Bartolomei, A., Salvadori, P.A., 2012. Analysis of image sharpness reproducibility on a novel engineered micro-CT scanner with variable geometry and embedded recalibration software. Phys. Med. 28, 166–173.
Peretto, C., Arnaud, J., Moggi-Cecchi, J., Manzi, G., Nomade, S., Pereira, A., Falguères, C., Bahain, J.J., Grimaud-Hervé, D., Berto, C., Sala, B., Lembo, G., Muttillo, B., Gallotti, R., Hohenstein, U.T., Vaccaro, C., Coltorti, M., Arzarello, M., 2015. A human deciduous tooth and new $^{40}Ar/^{39}Ar$ dating results from the Middle Pleistocene archaeological site of Isernia La Pineta, southern Italy. PLOS ONE 10, e0140091. http://dx.doi.org/10.1371/journal.pone.0140091.
Quam, R.M., Smith, F.H., 1998. A reassessment of the Tabun C2 mandible. In: Akazawa, T., Aoki, K., Bar-Yosef, O. (Eds.), Neandertals and modern humans in Western Asia. Plenum Press, New York, pp. 405–421.
Ramirez Rozzi, F.V., Bermudez de Castro, J.M., 2004. Surprisingly rapid growth in Neanderthals. Nature 428, 936–939.
Saunders, S.R., Chan, A.H.W., Kahlon, B., Kluge, H.F., FitzGerald, C.M., 2007. Sexual dimorphism of the dental tissues in human permanent mandibular canines and third premolars. Am. J. Phys. Anthropol. 133, 735–740.
Schwartz, G.T., 2000a. Taxonomic and functional aspects of the patterning of enamel thickness distribution in extant large-bodied hominoids. Am. J. Phys. Anthropol. 111, 221–244.
Schwartz, G.T., 2000b. Enamel thickness and the helicoidal wear plane in modern human mandibular molars. Arch. Oral Biol. 45, 401–409.
Schwartz, G.T., Dean, M.C., 2005. Sexual dimorphism in modern human permanent teeth. Am. J. Phys. Anthropol. 128, 312–317.
Skinner, M.M., Alemseged, Z., Gaunitz, C., Hublin, J.J., 2015. Enamel thickness trends in Plio-Pleistocene hominin mandibular molars. J. Hum. Evol. 85, 35–45.
Smith, B.H., 1984. Pattern of molar wear in hunter-gatherers and agriculturalists. Am. J. Phys. Anthropol. 63, 39–56.
Smith, T.M., Olejniczak, A.J., Martin, L.B., Reid, D.J., 2005. Variation in hominoid molar enamel thickness. J. Hum. Evol. 48, 575–592.
Smith, T.M., Olejniczak, A.J., Reid, D.J., Ferrell, R.J., Hublin, J.J., 2006. Modern human molar enamel thickness and enamel-dentine junction shape. Arch. Oral Biol. 51, 974–995.
Smith, T.M., Olejniczak, A.J., Reh, S., Reid, D.J., Hublin, J.J., 2008. Brief communication: Enamel thickness trends in the dental arcade of humans and chimpanzees. Am. J. Phys. Anthropol. 136, 237–241.
Smith, T.M., Toussaint, M., Reid, D.J., Olejniczak, A.J., Hublin, J.-J., 2007. Rapid dental development in a Middle Paleolithic Belgian Neanderthal. PNAS 104, 20220–20225.
Smith, T.M., Tafforeau, P., Reid, D.J., Pouech, J., Lazzari, V., Zermeno, J.P., Guatelli-Steinberg, D., Olejniczak, A.J., Hoffman, A., Radovčić, J., Makaremi, M., Toussaint, M., Stringer, C., Hublin, J.-J., 2010. Dental evidence for ontogenetic differences between modern humans and Neanderthals. PNAS 107, 20923–20928.
Smith, T.M., Olejniczak, A.J., Zermeno, J.P., Tafforeau, P., Skinner, M.M., Hoffmann, A., Radovcic, J., Toussaint, M., Kruszynski, R., Menter, C., Moggi-Cecchi, J., Glasmacher, U.A., Kullmer, O., Schrenk, F., Stringer, C., Hublin, J.J., 2012. Variation in enamel thickness within the genus *Homo*. J. Hum. Evol. 62, 395–411.
Thesleff, I., Keranen, S., Jernvall, J., 2001. Enamel knots as signaling centers linking tooth morphogenesis and odontoblast differentiation. Adv. Dent. Res. 15, 14–18.

Web references

ESRF database, http://paleo.esrf.eu/picture.php?/378/category/1509 (last accessed 23.07.17).
Seg3D v. 2.1.4 software, http://www.sci.utah.edu/cibc-software/seg3d.html (last accessed 23.07.17).
MEVISLAB Software, http://www.mevislab.de (last accessed 23.07.17).